Molecular Therapy
Original Article

Combining Constitutively Active Rheb Expression and Chondroitinase Promotes Functional Axonal Regeneration after Cervical Spinal Cord Injury

Di Wu,[1] Michelle C. Klaw,[1] Theresa Connors,[1] Nikolai Kholodilov,[2] Robert E. Burke,[2,3] Marie-Pascale Côté,[1] and Veronica J. Tom[1]

[1]Department of Neurobiology and Anatomy, Drexel University College of Medicine, Philadelphia, PA 19129, USA; [2]Department of Neurology, Columbia University, New York, NY, 10032 USA; [3]Department of Pathology and Cell Biology, Columbia University, New York, NY 10032, USA

After spinal cord injury (SCI), severed axons in the adult mammalian CNS are unable to mount a robust regenerative response. In addition, the glial scar at the lesion site further restricts the regenerative potential of axons. We hypothesized that a combinatorial approach coincidentally targeting these obstacles would promote axonal regeneration. We combined (1) transplantation of a growth-permissive peripheral nerve graft (PNG) into an incomplete, cervical lesion cavity; (2) transduction of neurons rostral to the SCI site to express constitutively active Rheb (caRheb; a Ras homolog enriched in brain), a GTPase that directly activates the growth-promoting pathway mammalian target of rapamycin (mTOR) via AAV-caRheb injection; and (3) digestion of growth-inhibitory chondroitin sulfate proteoglycans within the glial scar at the distal PNG interface using the bacterial enzyme chondroitinase ABC (ChABC). We found that expressing caRheb in neurons post-SCI results in modestly yet significantly more axons regenerating across a ChABC-treated distal graft interface into caudal spinal cord than either treatment alone. Excitingly, we found that caRheb+ChABC treatment significantly potentiates the formation of synapses in the host spinal cord and improves the animals' ability to use the affected forelimb. Thus, this combination strategy enhances functional axonal regeneration following a cervical SCI.

INTRODUCTION

After spinal cord injury (SCI), severed axons in the adult mammalian CNS are unable to robustly regenerate, leading to permanent functional deficiencies. This failure of axonal regeneration is attributed to an inhibitory environment in the CNS as well as a diminished intrinsic regenerative capacity of adult axons.[1–3] When provided with permissive substrates, such as a peripheral nerve graft (PNG), several populations of injured axons are capable of regenerating into and through the PNG. However, these axons stop abruptly at the distal graft-host interface because they encounter glial scar tissue.[4] After injury, astrocytes within the lesion penumbra undergo reactive gliosis; increase their production of growth-inhibitory molecules, including chondroitin sulfate proteoglycans (CSPGs); and contribute to the formation of the glial scar.[5–7] Notably, increased CSPGs in the glial scar appear to play a key role in the failure of axonal regeneration after injuries.[8] Digestion of scar-associated CSPGs by the bacterial enzyme chondroitinase ABC (ChABC), which cleaves the sugar moiety that confers inhibition from the protein core of CSPGs, improves regrowth of injured axons across the scarred boundary, including a distal PNG-host spinal cord interface. ChABC administration also promotes regenerating axons to synapse upon distal neurons and improves functional recovery after SCI.[9–12] To provide further impetus for axon growth out of the graft, we have explored combining ChABC administration at the distal PNG boundary with other strategies, including overexpression of the neurotrophin BDNF (brain derived neurotrophic factor) and pharmacological inhibition of the motor protein kinesin-5,[13,14] with some success.

More recently, we concurrently tackled both intrinsic and extrinsic obstacles by (1) grafting a PN to span a thoracic spinal transection site, (2) digesting the CSPGs at the distal PNG interface with ChABC, and (3) transducing neurons rostral to the SCI site to express constitutively active Rheb (caRheb; a Ras homolog enriched in brain).[15] Rheb is a small GTPase that directly activates mTOR when bound to GTP.[16] caRheb contains a point mutation that results in Rheb's being persistently bound to GTP and, consequently, continually activating mTOR.[17] Activation of mTOR is crucial for cell survival, proliferation, and augmenting axonal growth from different neuron populations after injuries.[18–22] Results in the previous studies demonstrated that caRheb expression and ChABC treatment of PNG interface had an additive effect and promoted more propriospinal axons to traverse across the PNG interface into caudal spinal cord, where they formed putative synapses, than either approach alone.[15] Although we found histological evidence that the regrown axons formed putative synapses upon host neurons, it was difficult for us to provide concrete

Received 31 May 2017; accepted 15 August 2017;
http://dx.doi.org/10.1016/j.ymthe.2017.08.011.

Correspondence: Veronica J. Tom, PhD, Department of Neurobiology and Anatomy, Spinal Cord Research Center, Drexel University College of Medicine, 2900 Queen Lane, Philadelphia, PA 19129, USA.
E-mail: veronica.tom@drexelmed.edu

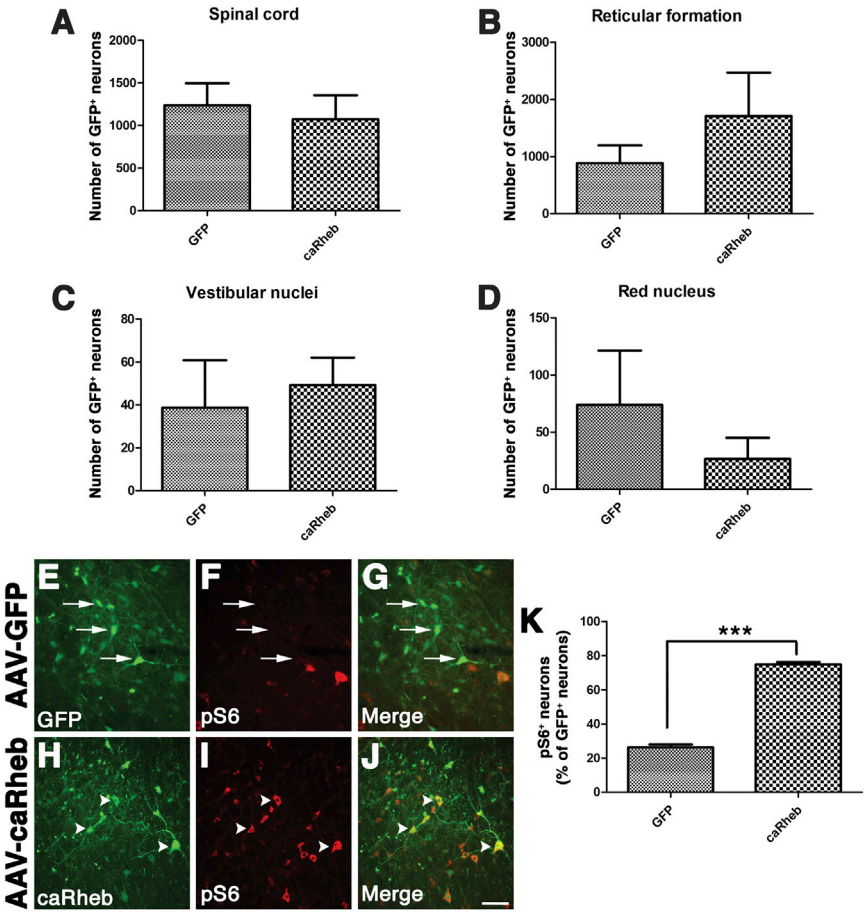

Figure 1. Quantification of Transduced Neurons within Spinal Cord and Brainstem following Intraspinal Injection of AAV-GFP or AAV-caRheb/GFP Rostral to a C2Hx

GFP^+ neurons in serially collected spinal cord and brain tissue sections from animals injected with either AAV5-GFP or AAV5-caRheb were manually counted. Many GFP^+ neurons were found in spinal cord and different brainstem regions. The total numbers of GFP^+ neurons in spinal cord (A), reticular formation (B), vestibular nuclei (C), and red nucleus (D) were compared for statistical significance between groups using Student's t test. There was no significant different between groups in any of the regions ($p > 0.05$). Representative images from spinal cord sections from rats receiving injections of AAV-GFP (E–G) or AAV-caRheb (H–J) that were stained for GFP (green) and pS6 (red). Many AAV-GFP transduced neurons (E and G, arrows) do not show immunoreactivity for pS6 (F and G, arrows). The merged image confirms that neurons expressing GFP control do not express pS6 (G). On the other hand, many AAV-caRheb transduced neurons (H and J, arrowheads) have high levels of pS6 (I and J, arrowheads). Quantification of the percentage of transduced, GFP^+ neurons in spinal cord that are also $pS6^+$ (K). Data are shown as mean ± SEM, n = 4, ***$p < 0.001$. Scale bar represents 100 μm.

evidence to indicate that axons that regenerated through the PNG synapsed with interneurons caudal to the injury site that mediate functional recovery, because of limitations with the transection injury model.

The neuron populations that grow axons into a PNG are highly dependent upon the level of injury, as the upregulation of regeneration-associated genes necessary for regrowth is linked to the distance of the injury from the cell body.[23] The closer the injury is to the soma, the greater the increase in regeneration-associated gene expression. As such, supraspinal neurons, such as the reticular formation and the red nucleus,[12] regenerate more readily into a cervical (C) graft than a thoracic (T) graft. Thoracic grafts are largely absent of descending axons and primarily contain propriospinal axons,[24] even when caRheb is expressed.[15] In the present study, we hypothesized that caRheb expression would provide more incentive for injured axons to grow beyond a ChABC-treated PNG and to reinnervate the spinal cord caudal to a cervical injury site. We adopted a similar strategy as in our previous study. We injected AAV5-caRheb rostral to a cervical level 2 hemisection (C2Hx) site to activate the mTOR pathway, provided a growth-supportive substrate within the injury site with a PNG bridge, and digested the inhibitory CSPGs at the distal PNG-spinal cord interface with ChABC. Anatomical, behavioral, and physiological assessments demonstrated that while this combinatorial treatment resulted in a moderate (yet significant) increase of axonal outgrowth from the graft, it significantly enhanced the ability of the axons that emerged from the graft to form functional synapses with host neurons and improved functional recovery.

RESULTS

Intraspinal AAV Injections Efficiently Transduce Neurons in Spinal Cord and Brain

Our previous study demonstrated that AAV5 injected into spinal cord tissue rostral to a thoracic transection site immediately after the injury is retrogradely transported and results in the transduction of a variety of neurons that project axons into spinal cord.[15,25] Because we use a cervical injury model here, we first wanted to characterize which neurons were transduced after injecting AAV5-GFP or AAV5-caRheb into ipsilateral spinal cord tissue rostral to a C2Hx site immediately after the lesion. Four weeks after the Hx and injections, we manually counted GFP^+ neurons in every other section of spinal cord rostral to C2 and in the brainstem.

As before, this technique resulted in robust transduction of neurons throughout spinal gray matter fairly close to the injection site (within ~5 mm). There were 1,237 ± 259.3 GFP^+ neurons in spinal cord injected with AAV-GFP and 1,073 ± 282.2 GFP^+ neurons in spinal cord injected with AAV5-caRheb (Figure 1A). Thousands

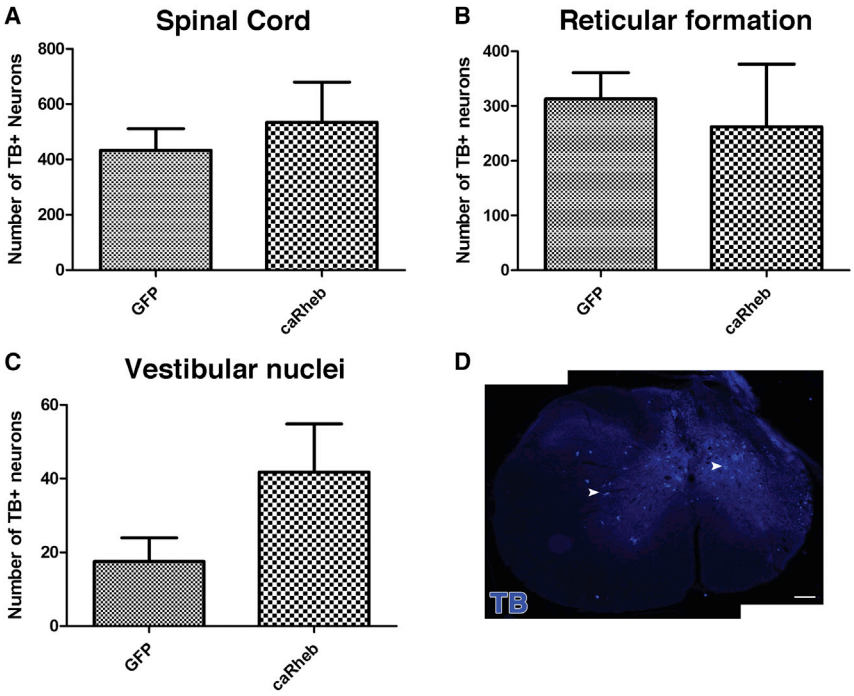

Figure 2. Retrograde Labeling of Neurons Projecting Axons into a Peripheral Nerve Graft

In animals injected with AAV5-GFP or AAV5-caRheb, the retrograde tracer True Blue was applied on the exposed distal end of PNGs to retrogradely label neurons whose axons reached the end of the PNG. In both groups, TB^+ neurons were identified in spinal cord gray matter (A), reticular formation (B), and vestibular nuclei (C). There was no significant difference in the number of TB^+ neurons between groups in spinal cord and both brain regions. An image of a representative section shows that the majority of TB^+ neurons in spinal cord rostral to the injury are located within the intermediate gray (D). Data are shown as mean ± SEM, n = 4. Scale bar represents 100 μm.

of GFP^+ neurons were also found within the brainstem (Figures 1B–1D). Statistically equal numbers of neurons within the reticular formation were transduced with AAV-GFP (884.5 ± 315.6) and AAV5-caRheb (1,708 ± 716.9) via the reticulospinal tract (Figure 1B). In the vestibular nucleus, we observed 38.75 ± 22.05 GFP-labeled neurons in AAV5-GFP injected animals and 49.25 ± 12.84 GFP-labeled neurons in AAV5-caRheb injected animals (Figure 1C). We also observed 73.75 ± 47.59 GFP labeled neurons in the red nucleus of animals injected with AAV-GFP and 26.5 ± 18.62 GFP^+ neurons in the red nucleus of animals injected with AAV5-caRheb (Figure 1D). We saw no significant differences in the number of GFP^+ neurons between the two animal groups in any of the regions. Thus, intraspinal injections of AAV5-GFP or AAV5-caRheb transduced neurons within the same regions at a similar efficiency.

To confirm that transducing neurons to express caRheb drove mTOR activity, we examined if there was an increased level of phosphorylated ribosomal protein S6 (pS6), a factor downstream of mTOR, via immunohistochemistry (Figures 1F and 1I). Spinal cord sections from animals that received AAV5-GFP (Figures 1E–1G) or AAV5-caRheb (Figures 1H–1J) were immunostained for pS6 and GFP. We noticed that in the animals that received AAV-GFP, many GFP^+ neurons (Figures 1E and 1G, arrows) had no pS6 immunoreactivity (Figures 1F, 1G, and 1K, arrows). On the other hand, strong pS6 immunoreactivity was detected in most $caRheb^+$ neurons (Figures 1H–1K, arrowheads). This caRheb-induced phosphorylation of pS6 is consistent with our previous observations in other injury models,[15,21] indicating that caRheb expression indeed activates mTOR.

caRheb Expression Does Not Increase the Number of Neurons Extending Axons into the PNG

Propriospinal neurons and some supraspinal neurons (including those in the red nucleus and the reticular formation) have the ability to regenerate axons into a PN grafted into a cervical lesion cavity.[12] We wanted to determine if expressing caRheb in propriospinal and supraspinal neurons improved regeneration of descending axons into a PNG after a C2Hx. To do so, AAV was injected rostral to a C2Hx, as above. Two weeks later, pre-degenerated PN was grafted into the Hx cavity. Four weeks later, the tracer True Blue (TB) was applied to the distal end of the PNG to retrogradely label neurons that regenerated axons into the graft.

As depicted in Figure 2, TB^+ neurons were found in the spinal cord gray matter (GFP 433 ± 78 versus caRheb 543 ± 145), mostly within the intermediate gray (Figure 2D, arrowheads). Although we observed TB^+ neurons primarily in the ipsilateral spinal cord, TB^+ neurons were identified in the contralateral spinal cord as well (Figure 2D). In the brainstem, TB^+ neurons were located in reticular formation (313 ± 48 versus 262 ± 114) and vestibular nuclei (18 ± 6 versus 42 ± 13) bilaterally. There was no significant difference in the number of neurons that extended axons in to the PNG between the AAV5-GFP and the AAV5-caRheb injection groups. Thus, the present data indicate that caRheb expression did not result in more neurons extending axons into the PNG after a C2Hx.

caRheb Expression Does Not Affect Axonal Growth into a PNG

Previous studies have reported that increasing activity of the mTOR pathway, including via caRheb expression, induces axonal sprouting in cervical spinal cord.[15,19,22] Moreover, we previously showed that whereas caRheb expression did not increase the number of neurons that extend into a PNG, it does increase sprouting and the number of axons within the PNG.[15] Therefore, it is possible that there are more axons growing into the PNG after caRheb expression than GFP control, despite caRheb expression's not having an effect on the total number of neurons that regenerate an axon into the PNG

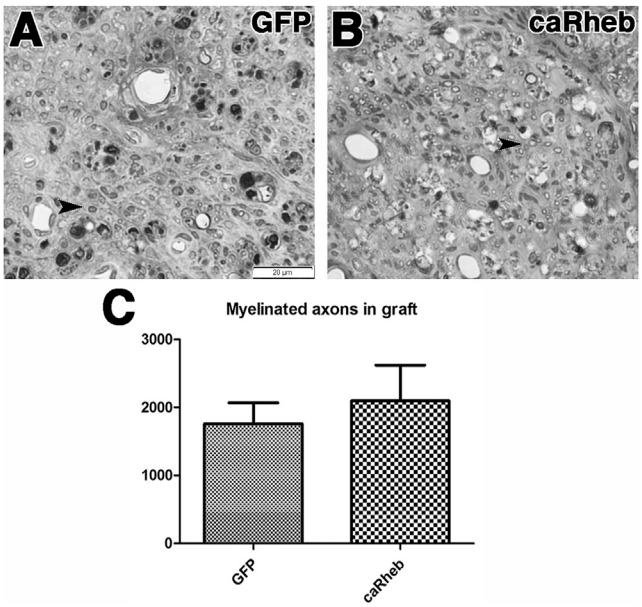

Figure 3. Quantification of Myelinated Axons in a PNG

Segments of PN that were grafted into the C2Hx sites from animals transduced with AAV-GFP (A, n = 4) or AAV-caRheb (B, n = 3) were processed for semithin sectioning to assess the number of myelinated axons that grew into the transplant. Many myelinated axons were found to have extended into the PNG in both groups (indicated by arrowheads). There was no statistical difference in the number of myelinated axons in PNG between groups (C). Mean ± SEM. Scale bar represents 20 μm.

(Figure 2). To assess if caRheb expression increases the number of regenerating axons in a PNG, AAV5-GFP or caRheb was injected above C2Hx. PNs were transplanted into the lesion cavity 2 weeks later. One month after grafting, PNGs were harvested. After semithin sections containing the grafts were processed to stain for myelinated axons, myelinated axons present in the PNG were counted. In both AAV5-GFP- and AAV5-caRheb-treated animals, there was considerable axonal regrowth into the PNGs (Figure 3). In the animals treated with AAV-GFP, 1,760 ± 308.2 myelinated axons were counted in the grafts (Figures 3A and 3C). With caRheb expression, there were 2,096 ± 525.9 myelinated axons in the graft (Figures 3B and 3C). This was statistically similar to the GFP control. Therefore, expressing caRheb in neurons after C2Hx injury did not significantly increase the sprouting or growth of axons into a PNG.

caRheb Enhances ChABC Mediated Axonal Regeneration beyond the Graft

It is well established that ChABC treatment of PNG-host spinal cord interface can digest the inhibitory CSPGs and allow axons that have extended throughout the PNG to grow beyond the graft. Here, we tested whether expressing caRheb in neurons further enhances this outgrowth. To specifically label the axons that grew through the PNG and into distal spinal cord tissue, 6 months after apposing the PNG into the C4DQ lesion, the PNG was cut in the middle and the distal end was immersed in BDA to diffusion-fill all (and only) axons within the graft. This approach eliminated the possibility of labeling axons that had sprouted into the gray matter ventral to the C4DQ lesion through spared pathways.

We observed that few BDA^+ axons extended into tissue ventral to the distal graft interface in animals that received PBS injections at the C4DQ site and either AAV-GFP (Figure 4A) or AAV-caRheb (Figure 4B). As demonstrated previously, after ChABC treatment of the graft-host interface, significantly more BDA^+ axons grew out of the PNG and were found throughout intermediate gray matter (Figures 4C–4E). We found significantly more BDA^+ regenerating axons in animals injected with AAV-caRheb+ChABC than in animals injected with AAV-GFP+ChABC, especially close to the ChABC-treated graft-host tissue boundary (i.e., within 100 μm; Figure 4E). In addition, we observed some BDA^+ axons beyond the intermediate gray matter and in the ventral horn region of the host spinal cord tissue. These data indicate that ChABC increased axonal regeneration beyond a PNG, as seen before. Excitingly, the expression of caRheb further enhanced this growth response.

caRheb Expression Enhances Electrical Stimulation-Induced c-Fos Expression in Host Spinal Cord

We wanted to determine if the enhanced regeneration beyond a PNG seen in the caRheb+ChABC animals translated into increased formation of functional synapses onto host neurons beyond the distal interface. In our previous studies, we were able to assess synapse formation by placing the PNG bridge that lies outside the spinal cord on a hook electrode to specifically stimulate regenerating axons within the graft.

We and others have used the immediate-early gene c-Fos as a marker of transsynaptic neuronal activation.[10,13,26,27] We counted the number of c-Fos neurons in host spinal cord after electrical stimulation of the PNG as an indicator of neurons that were synapsed upon by axons that grew out of the PNG.

We found, after stimulation of the PNG in the animals expressing GFP and treated with PBS, that there were very few neurons expressing c-Fos (4.18 ± 0.76 per section; Figures 5A and 5E). The rare neurons that were $c\text{-}Fos^+$ were located primarily in the ventral horn, far from the graft-host interface. Similarly, in sections from animals that were treated with PBS and AAV-caRheb, there were very few $c\text{-}Fos^+$ neurons ventral to the C4DQ apposition site (3.18 ± 0.40; Figures 5B and 5E). Conversely, there were significantly more neurons expressing c-Fos after electrical stimulation of the PNG in animals that were treated with ChABC and AAV5-GFP (9.0 ± 1.37; Figures 5C and 5E). These neurons were located fairly close to the graft (within 200 μm; Figure 5F). Expression of caRheb in the ChABC-treated animals resulted in a further increase in the number of $c\text{-}Fos^+$ neurons distal to the interface (26.45 ± 3.95; Figures 5D and 5E). As with the GFP+ChABC animals, these neurons were primarily located closer to the graft. However, there were significantly more $c\text{-}Fos^+$ neurons both close to the interface and at further distances (~400 μm; Figure 5F). This observation revealed that although caRheb expression alone was not able to promote axons to exit the graft, combining caRheb

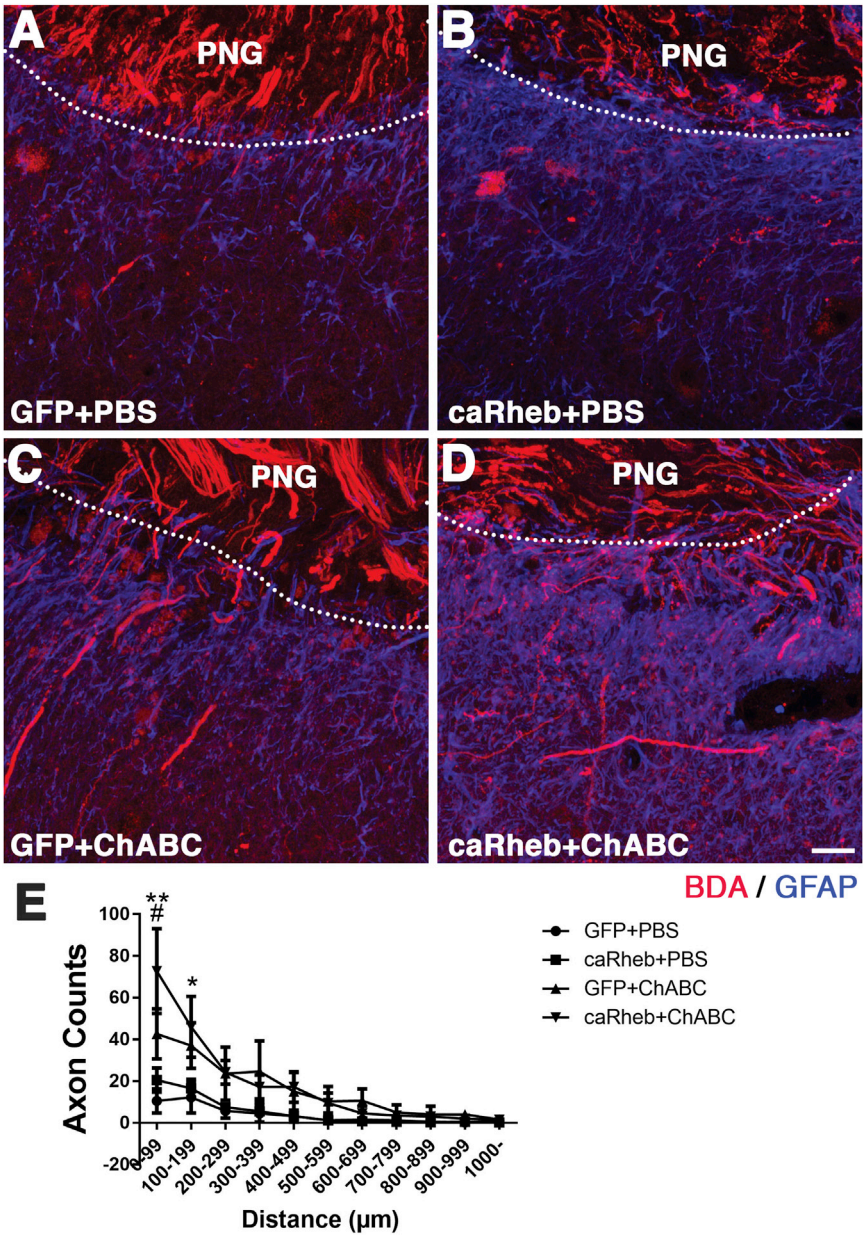

Figure 4. Axonal Regeneration Promoted by Combining caRheb Expression and ChABC Treatment

Axons within the graft were labeled with BDA. Representative images of transverse sections containing the PNG in the C4DQ were staining for BDA (red) and GFAP (blue). In animals treated with either GFP+PBS (A) or caRheb+PBS (B), few BDA-labeled axons grew beyond the graft-host interface (the boundary is denoted by the dashed lines surrounding the $GFAP^{-}$ peripheral nerve; quantified in E). On the other hand, significantly more BDA-labeled axons were found growing out of the PNG following ChABC treatment in GFP+ChABC animals (C and E). caRheb expression enhanced this ChABC-facilitated regeneration (D and E). Quantitative analysis revealed that both GFP+ChABC and caRheb+ChABC animals had significantly more axons within 200 μm distal to the PNG than animals treated with GFP+PBS or caRheb+PBS. Additionally, caRheb+ChABC animals had more axons than GFP+ChABC animals within 100 μm from the PNG-spinal cord interface (E). Data are shown as mean ± SEM; n = 4; *$p < 0.05$ and **$p < 0.01$, comparing ChABC-treated animals with PBS-treated animals; #$p < 0.05$, comparing caRheb+ChABC animals with GFP+ChABC animals. Scale bar represents 35 μm.

expression with ChABC treatment of the PNG interface enabled more axons to extend from the graft and enhanced synaptic efficacy of those axons.

Behavioral Results

Grooming Test

After C2Hx, we did not observe any differences in the animals' use of the contralateral (left) forelimb to groom.[28] This forelimb showed a normal grooming pattern that consisted of licking of the forepaws and rubbing of the mouth and nose, touching the eye region, and proceeding to the front and back of the ear, and eventually moving the paws back to the nose from the back of the head. In contrast, the right forelimb ipsilateral to the injury demonstrated a functional deficit throughout the duration of the study. In the first 6 weeks, the majority of the animals were only able to touch their chins (score of 1). From weeks 6–12, animals gradually improved their grooming ability. The contact area of the right front paw increased from the bottom of the snout to the eye region (score of 2). Most animals maintained the same degree of deficit for the remainder of the study, but a few animals continued to improve their grooming ability through week 20 (Figure 6A). Interestingly, this particular population of animals all received AAV-caRheb injection and ChABC treatment. This was the only group in which an animal achieved a score of 4 or above (Figures 6B and 6C). At the last three grooming test time points, these animals were able to contact the front of their ears with the affected forelimb while grooming, whereas the rest of the animals were not able to reach their ears with the ipsilateral front paws. These observations indicate that combining caRheb expression with ChABC treatment after C2Hx injury enhanced the recovery of the ability to use the affected forelimb to complete a grooming sequence.

CatWalk Analysis

We also assessed if combining AAV-caRheb injection and ChABC treatment affected the recovery of locomotor function in a CatWalk analysis. We detected a significant increase in the maximum contact maximum intensity in the caRheb+ChABC animals than the rest of

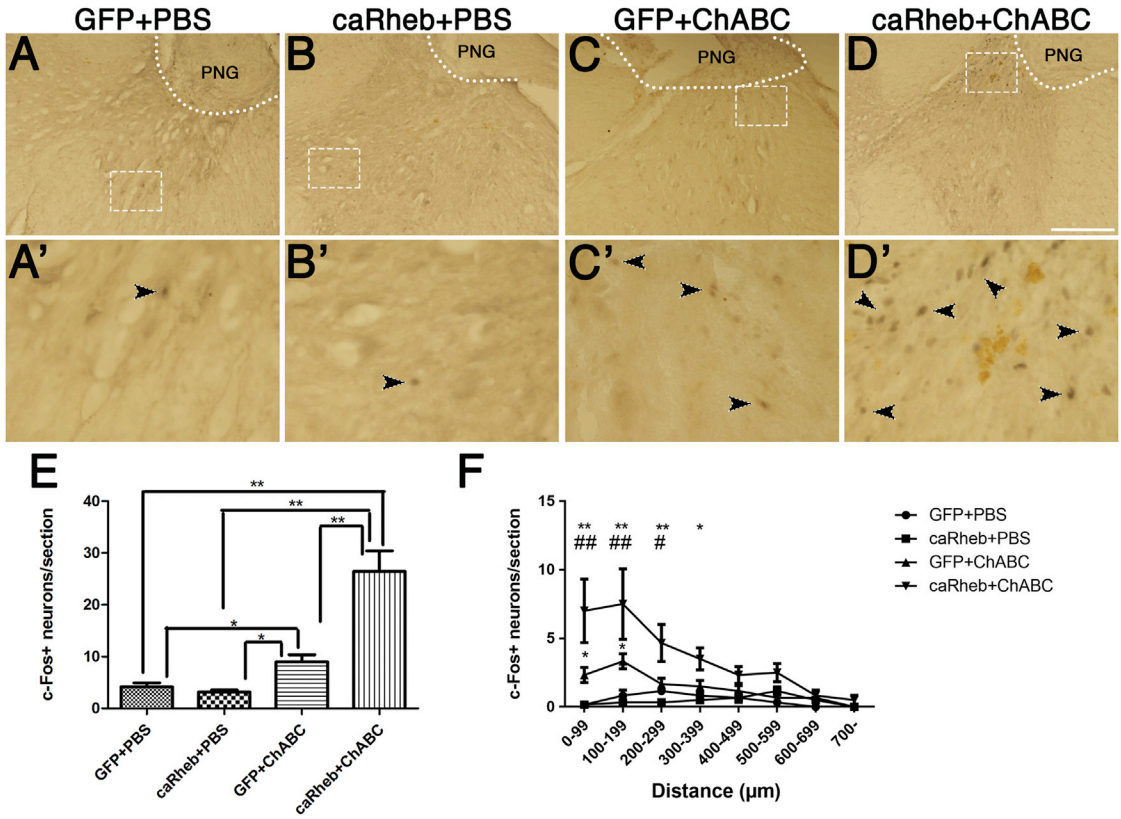

Figure 5. Induction of c-Fos in Host Neurons after Electrical Stimulation of Peripheral Nerve Graft

After electrical stimulation specifically of the PNG bridge, transverse sections containing the PN apposed to a C4DQ were processed for immunohistochemistry to visualize c-Fos expression. Animals that were treated with AAV-GFP+PBS (A) or AAV-caRheb+PBS (B) had few c-Fos$^+$ nuclei within gray matter. The inset boxes (A′ and B′) show high-magnification images of the boxed areas in (A) and (B). Arrowheads point out the c-Fos$^+$ nuclei in these sections. Significantly more c-Fos$^+$ nuclei were observed in host spinal cord tissue in AAV-GFP+ChABC-treated animals (C). Combining caRheb expression and ChABC treatment of the CSPG further increased the number of c-Fos$^+$ nuclei in spinal cord tissue ventral to the PNG (D). High-magnification image of boxed areas in (C) and (D) are shown in (C′) and (D′). Quantification and the result of one-way ANOVA of the number of c-Fos$^+$ nuclei in each group are shown in (E) (*$p < 0.05$, **$p < 0.01$; error bars represent SEM). The numbers of c-Fos$^+$ nuclei were binned to 100 μm intervals from the graft. (F) ChABC treatment increased the number of c-Fos$^+$ nuclei close to the graft interface, and caRheb expression further augmented this increase. Data are shown as mean ± SEM; n = 4; *$p < 0.05$ and **$p < 0.01$, comparing ChABC-treated animals with PBS-treated animals; #$p < 0.05$ and ##$p < 0.01$, comparing caRheb+ChABC-treated animals with GFP+ChABC-treated animals. Scale bar represents 250 μm.

the groups at week 24 (Figure 6C). These data suggest that at the last time point, animals that received the combinatorial treatment of caRheb expression and ChABC treatment put more weight on their injured paws when the paws were in full contact with the runway. We did not detect any differences between groups in speed and duration, step sequence regularity index, duration of the stance phase, and the duty cycle (data not shown).

DISCUSSION

SCI is a major challenge in clinical practice because injured adult CNS axons do not regenerate.[29] A limitation is that after neural circuits are established during development, intrinsic axonal growth potential is gradually diminished. Recently in the field, there has been a growing emphasis on using approaches to reactivate molecular programs that control axon growth to promote the growth of injured axons after injuries in the CNS.[30] Interestingly, it is possible to reverse the development-dependent decline of CNS neuron growth ability and return a mature neuron to a more growth permissive mode, to some extent.[3,31] Here, we hypothesized that transducing adult neurons rostral to a lesion site to express caRheb by injecting AAV in spinal cord rostral to the lesion site in combination with ChABC treatment of the glial scar would increase the injured axons' ability to grow through and out of a PNG and led to functional recovery. This hypothesis is based on a series of studies showing that activation of mTOR promotes CNS axons' intrinsic regenerative ability. For instance, deleting the known tumor suppressor gene PTEN enable axotomized retinal ganglion cells and corticospinal tract axons to regenerate.[19,32,33] PTEN is thought to inhibit growth by negatively regulating activation of mammalian target of rapamycin (mTOR). The mTOR pathway is well known for its ability to regulate protein synthesis related to cell growth and proliferation.[16] Deletion of PTEN leads to enhanced level of PIP3, activation of AKT, and activation of mTOR.

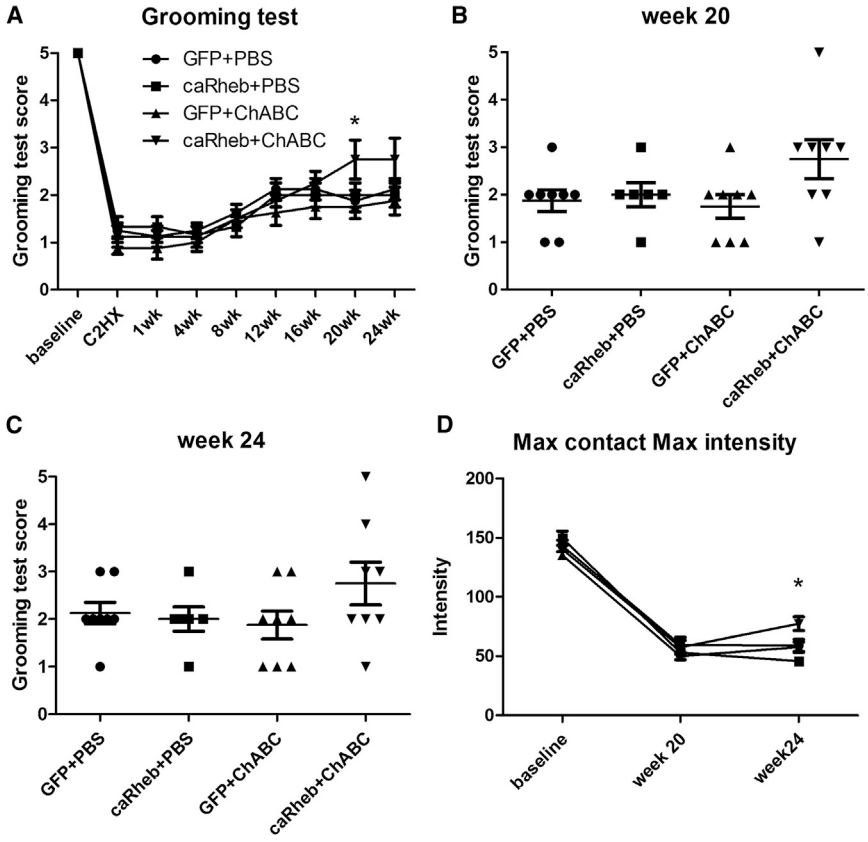

Figure 6. Forelimb Function Analyses after C2Hx Injuries

(A–C) The ability of C2Hx/C4DQ-injured animals to use their affected, ipsilateral forepaws to groom after AAV5-GFP+PBS, AAV5-caRheb+PBS, AAV5-GFP+ChABC, or AAV5-caRheb+ChABC treatment was assessed. The grooming test has a score range from 0–5, with 5 indicating full grooming capability. The C2Hx/C4DQ injuries detrimentally affected the animals' ability to use the ipsilateral forelimb to groom. The average scores were normalized and then compared between animal groups and across time points with a two-way ANOVA. At week 20, caRheb+ChABC animals had a significantly higher score than the other groups, including GFP+ChABC animals (A) ($n = 8$, $^*p < 0.05$). Grooming scores for individual animals at week 20 (B) and week 24 (C) (the last time point) are shown. The only animals that reached a score ≥ 4 after injury received both AAV5-caRheb and ChABC treatments. (D) Locomotor recovery analyzed using the CatWalk system revealed that by week 24, animals that received caRheb+ChABC had higher maximum contact maximum intensity than animals in any of the other groups. This indicates that the ipsilateral forepaw of AAV5-caRheb+ChABC animals has more contact with the runway because the animals are putting more weight on their injured forepaws when the injured paws have maximum contact with the glass (C). Data shown as mean ± SEM, $n = 8$, $^*p < 0.05$.

Previously, we found that transducing adult dorsal root ganglion neurons to express caRheb enhances synaptic integration of regenerated axons across a dorsal root entry zone (DREZ) following dorsal root crush.[21] We also found that expressing caRheb in propriospinal neurons rostral to a thoracic complete transection site in combination with ChABC treatment of the glial scar increases the injured axons' ability to grow through and out of a PNG and form putative synapses.[15] In the present study, we build upon our previous studies to determine if a similar strategy enhances axon regeneration and functional recovery after cervical SCI.

Our present study revealed that 1 month after apposing a PNG into a C2Hx site, expression of caRheb did not alter the total number of neurons that regenerated into the graft (Figure 2) or the number of myelinated axons present in the PNG (Figure 3). This is in contrast to the results of our previous study in which we observed that mTOR activation post-injury increased sprouting and extension of myelinated axons, primarily from propriospinal neurons, into a PN grafted into a T7 SCI site.[15] The discrepancy we observed between the two studies may be at least partially due to the difference of the injury levels. It is well established that injuries close to the cell body induce the expression of a more growth-permissive growth program than injuries far from the cell body.[23,24] Because axons extending into thoracic PNGs originate primarily from propriospinal neurons near the grafting site,[15,24] whereas those growing into a PN transplanted into a C2 lesion site come largely from supraspinal populations (e.g., reticular formation) far from the SCI site,[12] there are likely differential protein expression profiles within the two neuronal populations, even with caRheb expression. It will be necessary in future studies to determine if certain populations are more susceptible to caRheb/mTOR-enhanced sprouting or growth. Another possible explanation for why we failed to observe an increase of axon regeneration into the PNG after caRheb expression is the relatively short post-grafting survival period. In previous studies, PNGs were collected 6 months after grafting for semithin section analyses, whereas in the present study, we assessed axonal growth into a PNG 1 month after transplantation. When mTOR is activated after injury in adult animals, it may take substantially longer to observe an effect with mTOR activation on adult axon regeneration than neonatal axon regeneration. Indeed, Du et al.[22] found more chronically injured CST axons had regenerated across an SCI lesion site at 7 months than at 4 months after PTEN deletion, suggesting that these axons were still growing long after injury. We may speculate that at 1 month post-injury, animals from both groups projected similar amount of axons into a PNG, an extremely growth-supportive substrate. At a later time point, animals with caRheb expression may be able to extend more myelinated axons in PNG because of caRheb-enhanced growth. Correlating with this speculation, we did observe more regeneration in the caRheb+ChABC animals 6 months after PNG grafting (Figure 4).

Consistent with previous studies, although caRheb expression in adult rat neurons alone did not effectively promote axonal regeneration out of a PNG, combining neuronal caRheb expression and ChABC treatment of the glial scar moderately augmented the number of regenerating axons found in the host tissue beyond the graft-host interface. The mechanisms that stop axons at the distal interface are both intrinsic and extrinsic. Injured axons continue to express receptors, such as PTPσ and LAR, for growth-inhibitory CSPGs that are highly expressed at glial scar.[34,35] Here, we showed that after a C2Hx, caRheb expression can increase regeneration of injured axons out of the PNG only when the glial scar in host tissue is also treated with ChABC. This appears to hold true for other axon populations. Previously, we demonstrated that in a complete SCI model, axons from caRheb-expressing neurons can penetrate only a ChABC treated graft-spinal cord interface.[15] Similarly, when Lewandowski and Steward[32] used AAV-shPTEN to drive mTOR activity in rat sensorimotor cortical neurons, they did not observe enhanced CST sprouting or regrowth across a lesion site. It was only when they combined PTEN knockdown with salmon fibrin that they saw more CST fibers closer to the injury site, indicative of increased regrowth or diminished retraction. Last, only when caRheb expression is combined with NT-3 treatment or ChABC treatment do the central branches of rat DRG axons regenerate through DREZ and into spinal cord.[21,36] These studies suggest that activation of the mTOR signaling pathway more effectively induces regeneration when combined with other factors.

In addition to promoting axonal growth, caRheb expression has a significant and positive effect on the integration of regenerating axons. caRheb promotes synapse formation, as indicated by increased c-Fos expression in host neurons in the caRheb+ChABC animals after electrical stimulation of axons specifically within the PNG. Because most of the axons that extended into the graft are reticulospinal and propriospinal, populations that have previously been shown to be important for forming compensatory relay connections that mediate functional recovery,[37,38] this enhanced integration likely plays a role in the improved function we observed. It will be important in future studies to determine how to best shape this integration to enhance recovery.

We observed a similar enhancement with axons from caRheb-expressing DRGs that regenerated across a ChABC-treated DREZ following dorsal root crush.[21] Of interest, mTOR mediated protein synthesis has been previously suggested to participate in various aspects of synaptic functions, including increasing synaptic strength and affecting synapse number and synaptic vesicle number.[39] It was reported that mTOR activity regulates the balance between excitatory and inhibitory synaptic transmission.[40] Studies have also demonstrated that activation of mTOR by PTEN knockdown in vivo results in excitatory synapse formation with granule cells.[41] Likewise, inhibition of mTOR with rapamycin blocks excitatory synaptogenesis in the brain after epilepsy-induced synaptic reorganization.[42] However, though more and more evidence points to mTOR's playing an important role in synaptogenesis, maintaining synaptic homeostasis and synaptic output, the specific molecular mechanisms underlying mTOR's role in these activities remain unclear. One study suggests that mTOR suppresses dendritic translation of potassium channel Kv1.1, which leads to increased burst firing and has positive input in network synchronization.[43] Another study suggests that 4E-BP is a negative regulator of synaptic strength and that mTOR-dependent phosphorylation of 4E-BP counteracts this inhibition at the synapses, which then leads to increased synaptic strength.[44] These studies may provide mechanistic insight into how mTOR signaling influences synaptogenesis and synaptic homeostasis here.

One advantage of our treatment strategy is that we used AAV5 to limit the expression of caRheb to neurons. We have established that AAV5 with a non-cell-specific promoter predominantly transduces neurons in the brain and spinal cord and not glia.[25] Here, we demonstrated this neuronal specificity of AAV5 transduction again by evaluating the population of GFP^+ cells in brain and spinal cord (Figure 1). The neuronal specific expression of caRheb avoided the constitutive activation of mTOR in astrocytes. After CNS injuries, astrocytes become reactive and begin to build a glial scar barrier around the lesion cavity that prevents regenerative axon growth.[5,45] Activation of the PI3K/Akt/mTOR signaling pathway has been shown to be involved in the glial scar formation after SCI.[29,46] Therefore, although mTOR activation plays an important role in neuroprotection and axonal regeneration, it also facilitates astrocyte gliosis and the CSPG expression. On the other hand, attenuation of mTOR activation in astrocytes could modulate glial scar formation, which may lead to a permissive environment for neuronal regeneration and improved locomotor recovery following SCI.[46] The present study showed the possibility of preferentially regulating mTOR activation in neurons to allow concurrent enhancement of the intrinsic regenerative ability in neurons and the modulation of extracellular matrix deposited from activated astrocytes within the glial scar. Another advantage of this strategy is its specificity. Rheb is a direct activator of mTOR and exclusively activates the mTOR pathway without affecting other signaling pathways.[47,48] On the other hand, PTEN deletion activates neuronal protein synthesis through both mTOR-dependent and mTOR-independent mechanisms.[49] PTEN regulation of both the PI3K/Akt/mTOR and PI3K/Akt/GSK3β pathways has been implicated in cancer.[50,51] Therefore, an exclusive and direct activation of mTOR specifically in post-mitotic CNS neurons is less likely to trigger untoward effects. However, further systematic studies of the physiological consequences of prolonged mTOR activation in the CNS are needed to fully evaluate safety.

In conclusion, we found that AAV-mediated expression of caRheb in adult neurons enhanced axonal regeneration out of a PN grafted into a cervical injury when combined with ChABC digestion of CSPGs present within the glial scar. More importantly, caRheb significantly potentiated synapse formation of these axons with host spinal neurons, indicating caRheb expression can be used to maximize the effects of a limited number of regenerating axons. The increased functional regeneration correlated with improved behavioral recovery, suggesting that it may elucidate the basis for a treatment strategy to promote functional recovery after SCI.

MATERIALS AND METHODS

Animals

Adult female Fischer 344 rats (150–200 g; Charles River) were used for these experiments. All procedures complied with Drexel University's Institutional Animal Care and Use Committee and NIH guidelines for the care and use of laboratory animals. Animals were allowed to acclimate for a least 1 week after arrival before any procedure was done. After all survival surgeries, animals were given 5 mL lactated Ringer's solution, ampicillin (200 mg/kg), and slow-release buprenorphine (0.1 mg/kg) and placed on a thermal barrier to recover.

Preparation of the PN for Grafting into a C2Hx Site

One week after C2Hx surgery, the tibial nerves of donor rats were ligated and cut. One week later, donor rats were anesthetized with intraperitoneally injection of ketamine (60 mg/kg) and xylazine (10 mg/kg). Pre-degenerated tibial nerve was removed immediately before grafting.

C2Hx SCI, AAV Injection, and Grafting of the Proximal End of the PN

Animals were anesthetized with isoflurane and kept on a heating pad to prevent hypothermia. Under aseptic technique, the dorsal surface of C2 was exposed by laminectomy. A small slit was made in the overlying dura using a micro knife. A complete unilateral Hx lesion cavity was created by aspiration in all animals.

In addition, 1 μL of AAV5 was slowly injected into ipsilateral spinal cord at five locations 1 mm rostral to the Hx site using a Hamilton syringe with a pulled glass micropipette. Animals in the caRheb group received injection of a mixture of AAV5-CBA-GFP and AAV5-CBA-caRheb (final titer of 1.6×10^9 genomic copies (GC)/μL for each vector; termed AAV5-caRheb for brevity's sake), and animals in the GFP group received AAV5-CBA-GFP at a final titer of 1.6×10^9 GC/μL. The technique of intraspinal injection was similar to that described previously.[15,25] Overlying musculature and skin were then closed.

Two weeks after C2Hx and AAV injection, rats were anesthetized with isoflurane. The C2Hx site was exposed, and the overlying dura was opened with forcipes carefully. The fibrotic tissue within the lesion cavity was gently removed by aspiration. Special care was taken to not remove spinal cord tissue spared from the initial C2Hx.

A pre-degenerated tibial nerve from a donor animal (~15 mm in length; see above) was harvested. The perineurium from the proximal end of the pre-degenerated tibial nerve was peeled. The proximal end of the PNG was placed into the C2 cavity, and the perineurium was sutured to the dura to secure the graft. The distal end of the graft was left free outside the spinal column and wrapped with BioBrane Silastic membrane. Then, the overlying musculature and skin was closed.

Grafting a PN to "Bridge" a C2Hx and C4 Dorsal Quadrant Lesions

The grafting procedure is similar to that described previously.[10,12,13] Four weeks after grafting the proximal end of a PN into a C2Hx site, animals were anesthetized with isoflurane. A laminectomy was performed on the right side of spinal cord at the level of C4. The dura was cut open and the dorsal quadrant (DQ) was aspirated out to create a 1 mm lesion. At this time point, injured axons that extended into the PNG had had enough time to grow through the graft to reach the distal end. By apposing the distal end of the PNG to the C4DQ site at this time, the potential for actively regenerating axons within the graft to exit the graft and integrate with tissue is maximized. Half of the animals were injected with 0.5 μL PBS vehicle immediately rostral, caudal, and ventral to the fresh DQ lesion. The remaining animals were injected with ChABC (50 U/mL; AMS Biotechnology) to digest CSPGs. The free distal end of the PNG was trimmed by 1 mm and placed into the C4DQ cavity. This distal graft end was secured by suturing the perineurium to the dura mater and covered with BioBrane membrane (UDL Laboratories). The overlying musculature was sutured, and the skin was closed using wound clips. In total, we had four groups: AAV-GFP+PBS (n = 18), AAV-caRheb+PBS (n = 19), AAV-GFP+ChABC (n = 19), and AAV-caRheb+ChABC (n = 18).

TB Retrograde Labeling

To identify the neurons whose axons regenerated into the PNG, a separate cohort of animals received C2Hx lesion, virus injection (n = 4 for AAV5-GFP and n = 4 for AAV5-caRheb), and PN grafting into the C2Hx site, as described above. Four weeks after placing the proximal end of a PN graft into the C2Hx lesion site, the distal end of PN graft was exposed, trimmed by at least 1 mm, and exposed to GELFOAM saturated with 2% TB (Sigma-Aldrich). Animals were euthanized 1 week later by an overdose of Euthasol, then perfused transcardially with ice-cold 0.9% saline followed by ice-cold 4% paraformaldehyde (PFA). Spinal cord and brain tissues were dissected out, postfixed in 4% PFA overnight at 4°C, and cryoprotected in 30% sucrose.

The entire brainstem and spinal cord rostral to the C2Hx lesion was sectioned in a coronal plane at a thickness of 50 μm. Every other section was mounted serially onto glass slides, dried, and coverslipped with Fluoromount (Biomedical Specialties). To characterize the transduction efficiency and which neurons regenerated axons into the PNG, each mounted section was examined by fluorescence microscopy to detect the number and location of supraspinal and propriospinal neurons that were labeled with GFP and TB, respectively. The number of GFP^+ and TB^+ neurons in a specific region in each section was manually counted while blinded to treatment and subsequently summed for each animal and compared for significance using Student's t test ($p < 0.05$ was the criterion for significance).

pS6 Expression in AAV-Transduced Neurons

To verify that expressing caRheb activates mTOR signaling pathways in neurons expressing caRheb, spinal cord sections rostral to C2Hx from animals injected with AAV5-GFP or the mixture of AAV5-caRheb coronal sections from spinal cord rostral to C2Hx were immunostained for pS6 and GFP. Sections were blocked in 5% normal goat serum and 10% BSA with 0.1% Triton X-100 in PBS

for 1 hr. After blocking, sections were incubated with primary antibodies anti-GFP (1:500; Millipore) and anti-phosphorylated ribosomal pS6 (1:800; Cell Signaling Technology) at 4°C overnight. The next day, sections were washed, incubated with appropriate Alexa Fluor-conjugated secondary antibodies (1:500; Invitrogen) for 2 hr, washed in PBS, mounted onto slides, and coverslipped with FluorSave (EMD Chemical). All sections were processed at the same time, and images for all sections were acquired using the Leica DM5500B epifluorescent microscopes with the same exposure time.

Semithin Sections

To quantify the number of axons that grew into the PNGs, a portion from the middle of the grafts from animals injected with AAV5-GFP (n = 3) or AAV5-caRheb (n = 4) was processed for plastic-embedded, semithin sectioning, as done previously.[10,15] Briefly, 1 month after grafting a PN into a C2Hx site, animals were perfused with 4% PFA, and the grafts were dissected out and postfixed overnight. The grafts were then kept in 0.1 M phosphate buffer until embedding. On the day before embedding, the grafts were treated with 1% osmium tetroxide, rinsed in PBS, and stained in 2% uranyl acetate. The tissue was then washed and dehydrated in a series of ascending graded alcohols from 70% to 100%. After that, the tissue was immersed in propylene oxide and then incubated in a 2:1 solution of Epon/propylene oxide overnight. The following day, the tissue was placed flat into a mixture of Epon-812 and Araldite in silicone molds. The molds with the grafts were placed in a 60°C oven for 3 days to polymerize the plastic. All materials were obtained from Electron Microscopy Sciences. After embedment, grafts were trimmed and cut into transverse sections on a Reichert ultramicrotome at a thickness of 1 μm.

Myelinated axons were quantified with ImageJ (NIH) using well-established methodology.[15,52,53] High magnification (40×) bright-field images were captured using an Olympus BX51 microscope and stitched together to allow visualization of the entire transverse sections of the PNG. Myelinated axons were manually counted in equivalently sized and similarly located regions from each PNG section as described before. The average density of myelinated axons was determined and used to calculate a total number of myelinated axons per graft, on the basis of the total size of the graft. The total numbers of axons in the PNG were compared using Student's t test. Significance was determined at $p < 0.05$.

Behavioral Analyses

Baseline scores for all behavioral analyses were obtained before animals received the C2Hx and then again before the C4DQ injury. After the C4DQ lesion and completion of the PNG "bridge," animals' behavioral activity was assessed biweekly for 6 months.

CatWalk Gait Analysis

For quantitative assessment of footfalls and motor performance after C2Hx, all animals were placed in a CatWalk XT system.[54] Rats were trained to walk across a Plexiglas plate voluntarily toward a goal box, where their footprints were captured by a high-speed camera placed underneath. CatWalk software NXT v.10.5 (Noldus Information Technologies) was used to visualize the foot prints and calculate statistics related to print dimensions and the time and distance relationships between footfalls. Animals were pre-trained for 5 days prior to the baseline test and tested every other week until the end of the experiment. Speed, step sequence, swing, stand, duty cycle, maximum contact at percentage, and maximum contact maximal intensity were analyzed for detecting locomotion functional recovery. Paw statistics were compared using two-way ANOVA. The factors were treatment and time with repeated measures on different time points. Bonferroni post-test was used for post hoc analysis ($p < 0.05$ was the criterion for significance; GraphPad Prism v.5).

Grooming Test

We assessed the animals' ability to use the right forelimb to perform a stereotyped motion to groom the head and face.[28] To induce the grooming behavior, cool tap water was applied to the animal's head and back with paper towel, and the animal was returned to its home cage. Each animal's movements were recorded with a video camera so that we could score the recovery of forelimb function using slow-motion video playback.

On each test day, we recorded at least two stereotypical grooming sequences for each animal. A grooming sequence includes (1) licking of the forepaws and face washing, (2) forelimb grooming of the face, (3) repetitive licking of the body, and (4) hindpaw scratching. The ability of the animal to use the ipsilateral, affected forepaw to groom was scored using the following scale:[28] 0 if the animal was unable to contact any part of the face or head, 1 if the animal's forepaw touched the underside of the chin and/or the mouth area, 2 if the animal's forepaw contacted the area between the nose and the eye, 3 for the animal's forepaw contacted the eyes and the area up to but not including the front of the ears, 4 if the animal's forepaw contacted the front but not the back of the ear, and 5 if the animal's forepaw contacted the area of the head behind the ears. Because the grooming test is scaled, the distribution of the population violates the assumption of normality for two-way ANOVA. Thus, we first transformed the data using the built-in function in GraphPad Prism v.5. The normalized data were then analyzed using two-way ANOVA followed by post hoc Tukey's tests ($p < 0.05$ was the criterion for significance).

Labeling of Regenerating Axons in PNG

After the last behavior test (6 months after the C4DQ lesion and PN graft apposition), 20 animals (n = 5 for each experimental group) were used to trace the axons that regenerated into and beyond the PNG. Animals were anesthetized with isoflurane, and the graft was exposed. The graft was cut at its midpoint, and the distal end was soaked with 10% biotinylated dextran amine (BDA) to diffusion-fill axons within the PNG, as done previously.[10,12,13] Axons growing through the PNG and extending beyond of the distal PNG interface were anterogradely labeled. Animals were perfused 1 week later with 4% PFA. Brains and spinal cord were dissected, post-fixed in 4% PFA, and subsequently cryoprotected in 30% sucrose. Twenty-five-micrometer transverse sections of C3–C5 spinal cord were cut

on a cryostat and collected in a series of six sets. To visualize BDA-labeled axons, sections were blocked in 5% normal goat serum, 1% BSA, and 0.1% Triton X-100 in PBS for 1 hr at room temperature, followed by incubation with Alexa 594 conjugated to avidin (Invitrogen). Sections were also incubated with anti-glial fibrillary acidic protein (GFAP; Dako) to visualize astrocytes in host spinal cord. After staining was completed, they were mounted on glass slides using Fluoromount and coverslipped.

Sections containing the PNG were examined using an Olympus BX51 microscope that had an ocular micrometer while blinded to treatment. Regenerating axons beyond the graft-host interface were counted and binned into ten categories on the basis of the distance they traveled beyond to the most ventral point of graft edge in 100 μm intervals. The numbers of axons per distance in each section were summed for each rat subset. The numbers of axons at each length among the four groups of animals were compared for statistical significance using one-way ANOVA followed by Bonferroni correction ($p < 0.05$ was the criterion for significance; GraphPad Prism v.5).

Electrical Stimulation of the PNG

Another 20 animals (n = 5 per experimental group) were anesthetized with ketamine and xylazine after the last behavioral test. As conducted previously,[10,13] the PNG "bridge" was exposed and dissected free from surrounding tissues. The graft was lifted up and placed onto a bipolar hook electrode for stimulation. The nerves were bathed in a pool of mineral oil to prevent desiccation of the nerves throughout the stimulation period. The nerve was stimulated for 1 hr using 1 mA amplitude, 100 μs pulse duration and 50 Hz frequency. Animals were perfused 2 hr later with ice-cold 0.9% saline followed by ice-cold 4% PFA. The spinal cords with PNG attached were dissected out, postfixed in the same fixative overnight at 4°C, and cryoprotected in 30% sucrose for at least 48 hr. C3–C5 spinal cord tissues were embedded in OCT and cut into 25 μm coronal sections. Sections were collected serially and blocked in 5% normal goat serum and 10% BSA with 0.1% Triton X-100 in PBS for 1 hr and then incubated with anti-c-Fos (Santa Cruz) at 4°C overnight. The next day, sections were washed, incubated with appropriate biotin-conjugated secondary antibodies for 2 hr, washed, and then incubated with avidin-HRP, rinsed again, and processed using 3'-diaminobenzidine (DAB). Sections were washed in PBS, mounted onto slides, dehydrated, and coverslipped.

To quantify the number of c-Fos-positive cells, images of transverse sections of C4 spinal cord containing the apposed PNG that were stained with anti-c-Fos were taken with a Leica DM5500B microscope. All images were subjected to the same saturation threshold level to eliminate background. c-Fos$^+$ neurons in gray matter ipsilateral to the graft were counted in each section (n = 4 sections per animal). The average number of ipsilateral c-Fos$^+$ neurons per section was calculated and compared among groups. The statistical analysis was performed with one-way ANOVA and post hoc Tukey's test (GraphPad Prism). A p value < 0.05 was considered to indicate statistical significance.

AUTHOR CONTRIBUTIONS

D.W. and V.J.T. designed the experiments. D.W., M.C.K., T.C., and M.-P.C. performed the research. N.K. and R.E.B. contributed reagents. D.W. and V.J.T. analyzed the data and wrote the paper.

CONFLICTS OF INTEREST

The authors declare no conflict of interest.

ACKNOWLEDGMENTS

This work was funded by NIH grants R01 NS085426 (to V.J.T.) and P50 NS038370 (to R.E.B.). The authors gratefully acknowledge the use of core facilities within the Drexel University Spinal Cord Research Center and Dr. Vladimir Zhukarev's assistance with the confocal microscope.

REFERENCES

1. Schwab, M.E., and Bartholdi, D. (1996). Degeneration and regeneration of axons in the lesioned spinal cord. Physiol. Rev. *76*, 319–370.
2. Harel, N.Y., and Strittmatter, S.M. (2006). Can regenerating axons recapitulate developmental guidance during recovery from spinal cord injury? Nat. Rev. Neurosci. *7*, 603–616.
3. Liu, K., Tedeschi, A., Park, K.K., and He, Z. (2011). Neuronal intrinsic mechanisms of axon regeneration. Annu. Rev. Neurosci. *34*, 131–152.
4. Ye, J.H., and Houle, J.D. (1997). Treatment of the chronically injured spinal cord with neurotrophic factors can promote axonal regeneration from supraspinal neurons. Exp. Neurol. *143*, 70–81.
5. Fitch, M.T., and Silver, J. (2008). CNS injury, glial scars, and inflammation: inhibitory extracellular matrices and regeneration failure. Exp. Neurol. *209*, 294–301.
6. Lemons, M.L., Howland, D.R., and Anderson, D.K. (1999). Chondroitin sulfate proteoglycan immunoreactivity increases following spinal cord injury and transplantation. Exp. Neurol. *160*, 51–65.
7. Wanner, I.B., Anderson, M.A., Song, B., Levine, J., Fernandez, A., Gray-Thompson, Z., Ao, Y., and Sofroniew, M.V. (2013). Glial scar borders are formed by newly proliferated, elongated astrocytes that interact to corral inflammatory and fibrotic cells via STAT3-dependent mechanisms after spinal cord injury. J. Neurosci. *33*, 12870–12886.
8. Galtrey, C.M., and Fawcett, J.W. (2007). The role of chondroitin sulfate proteoglycans in regeneration and plasticity in the central nervous system. Brain Res. Brain Res. Rev. *54*, 1–18.
9. Barritt, A.W., Davies, M., Marchand, F., Hartley, R., Grist, J., Yip, P., McMahon, S.B., and Bradbury, E.J. (2006). Chondroitinase ABC promotes sprouting of intact and injured spinal systems after spinal cord injury. J. Neurosci. *26*, 10856–10867.
10. Tom, V.J., Sandrow-Feinberg, H.R., Miller, K., Santi, L., Connors, T., Lemay, M.A., and Houlé, J.D. (2009). Combining peripheral nerve grafts and chondroitinase promotes functional axonal regeneration in the chronically injured spinal cord. J. Neurosci. *29*, 14881–14890.
11. Bradbury, E.J., Moon, L.D., Popat, R.J., King, V.R., Bennett, G.S., Patel, P.N., Fawcett, J.W., and McMahon, S.B. (2002). Chondroitinase ABC promotes functional recovery after spinal cord injury. Nature *416*, 636–640.
12. Houle, J.D., Tom, V.J., Mayes, D., Wagoner, G., Phillips, N., and Silver, J. (2006). Combining an autologous peripheral nervous system "bridge" and matrix modification by chondroitinase allows robust, functional regeneration beyond a hemisection lesion of the adult rat spinal cord. J. Neurosci. *26*, 7405–7415.
13. Tom, V.J., Sandrow-Feinberg, H.R., Miller, K., Domitrovich, C., Bouyer, J., Zhukareva, V., Klaw, M.C., Lemay, M.A., and Houlé, J.D. (2013). Exogenous BDNF enhances the integration of chronically injured axons that regenerate through a peripheral nerve grafted into a chondroitinase-treated spinal cord injury site. Exp. Neurol. *239*, 91–100.
14. Xu, C., Klaw, M.C., Lemay, M.A., Baas, P.W., and Tom, V.J. (2015). Pharmacologically inhibiting kinesin-5 activity with monastrol promotes axonal regeneration following spinal cord injury. Exp. Neurol. *263*, 172–176.

15. Wu, D., Klaw, M.C., Connors, T., Kholodilov, N., Burke, R.E., and Tom, V.J. (2015). Expressing constitutively active Rheb in adult neurons after a complete spinal cord injury enhances axonal regeneration beyond a chondroitinase-treated glial scar. J. Neurosci. *35*, 11068–11080.

16. Durán, R.V., and Hall, M.N. (2012). Regulation of TOR by small GTPases. EMBO Rep. *13*, 121–128.

17. Kim, S.R., Kareva, T., Yarygina, O., Kholodilov, N., and Burke, R.E. (2012). AAV transduction of dopamine neurons with constitutively active Rheb protects from neurodegeneration and mediates axon regrowth. Mol. Ther. *20*, 275–286.

18. Park, K.K., Liu, K., Hu, Y., Smith, P.D., Wang, C., Cai, B., Xu, B., Connolly, L., Kramvis, I., Sahin, M., and He, Z. (2008). Promoting axon regeneration in the adult CNS by modulation of the PTEN/mTOR pathway. Science *322*, 963–966.

19. Liu, K., Lu, Y., Lee, J.K., Samara, R., Willenberg, R., Sears-Kraxberger, I., Tedeschi, A., Park, K.K., Jin, D., Cai, B., et al. (2010). PTEN deletion enhances the regenerative ability of adult corticospinal neurons. Nat. Neurosci. *13*, 1075–1081.

20. Zhou, S., Shen, D., Wang, Y., Gong, L., Tang, X., Yu, B., Gu, X., and Ding, F. (2012). microRNA-222 targeting PTEN promotes neurite outgrowth from adult dorsal root ganglion neurons following sciatic nerve transection. PLoS ONE *7*, e44768.

21. Wu, D., Klaw, M.C., Kholodilov, N., Burke, R.E., Detloff, M.R., Côté, M.P., and Tom, V.J. (2016). Expressing constitutively active Rheb in adult dorsal root ganglion neurons enhances the integration of sensory axons that regenerate across a chondroitinase-treated dorsal root entry zone following dorsal root crush. Front. Mol. Neurosci. *9*, 49.

22. Du, K., Zheng, S., Zhang, Q., Li, S., Gao, X., Wang, J., Jiang, L., and Liu, K. (2015). Pten deletion promotes regrowth of corticospinal tract axons 1 year after spinal cord injury. J. Neurosci. *35*, 9754–9763.

23. Tetzlaff, W., Kobayashi, N.R., Giehl, K.M., Tsui, B.J., Cassar, S.L., and Bedard, A.M. (1994). Response of rubrospinal and corticospinal neurons to injury and neurotrophins. Prog. Brain Res. *103*, 271–286.

24. Richardson, P.M., Issa, V.M., and Aguayo, A.J. (1984). Regeneration of long spinal axons in the rat. J. Neurocytol. *13*, 165–182.

25. Klaw, M.C., Xu, C., and Tom, V.J. (2013). Intraspinal AAV injections immediately rostral to a thoracic spinal cord injury site efficiently transduces neurons in spinal cord and brain. Mol. Ther. Nucleic Acids *2*, e108.

26. Bonner, J.F., Connors, T.M., Silverman, W.F., Kowalski, D.P., Lemay, M.A., and Fischer, I. (2011). Grafted neural progenitors integrate and restore synaptic connectivity across the injured spinal cord. J Neurosci. *31*, 4675–4686.

27. Landrum, L.M., Jones, S.L., and Blair, R.W. (2002). The expression of Fos-labeled spinal neurons in response to colorectal distension is enhanced after chronic spinal cord transection in the rat. Neuroscience. *110*, 569–578.

28. Gensel, J.C., Tovar, C.A., Hamers, F.P., Deibert, R.J., Beattie, M.S., and Bresnahan, J.C. (2006). Behavioral and histological characterization of unilateral cervical spinal cord contusion injury in rats. J. Neurotrauma *23*, 36–54.

29. Luan, Y., Chen, M., and Zhou, L. (2017). MiR-17 targets PTEN and facilitates glial scar formation after spinal cord injuries via the PI3K/Akt/mTOR pathway. Brain Res. Bull. *128*, 68–75.

30. Yang, P., and Yang, Z. (2012). Enhancing intrinsic growth capacity promotes adult CNS regeneration. J. Neurol. Sci. *312*, 1–6.

31. Mar, F.M., Bonni, A., and Sousa, M.M. (2014). Cell intrinsic control of axon regeneration. EMBO Rep. *15*, 254–263.

32. Lewandowski, G., and Steward, O. (2014). AAVshRNA-mediated suppression of PTEN in adult rats in combination with salmon fibrin administration enables regenerative growth of corticospinal axons and enhances recovery of voluntary motor function after cervical spinal cord injury. J. Neurosci. *34*, 9951–9962.

33. Zukor, K., Belin, S., Wang, C., Keelan, N., Wang, X., and He, Z. (2013). Short hairpin RNA against PTEN enhances regenerative growth of corticospinal tract axons after spinal cord injury. J. Neurosci. *33*, 15350–15361.

34. Li, H., Wong, C., Li, W., Ruven, C., He, L., Wu, X., Lang, B.T., Silver, J., and Wu, W. (2015). Enhanced regeneration and functional recovery after spinal root avulsion by manipulation of the proteoglycan receptor PTPσ. Sci. Rep. *5*, 14923.

35. Shen, Y., Tenney, A.P., Busch, S.A., Horn, K.P., Cuascut, F.X., Liu, K., He, Z., Silver, J., and Flanagan, J.G. (2009). PTPsigma is a receptor for chondroitin sulfate proteoglycan, an inhibitor of neural regeneration. Science *326*, 592–596.

36. Liu, Y., Kelamangalath, L., Kim, H., Han, S.B., Tang, X., Zhai, J., Hong, J.W., Lin, S., Son, Y.J., and Smith, G.M. (2016). NT-3 promotes proprioceptive axon regeneration when combined with activation of the mTor intrinsic growth pathway but not with reduction of myelin extrinsic inhibitors. Exp. Neurol. *283* (Pt A), 73–84.

37. Filli, L., Engmann, A.K., Zörner, B., Weinmann, O., Moraitis, T., Gullo, M., Kasper, H., Schneider, R., and Schwab, M.E. (2014). Bridging the gap: a reticulo-propriospinal detour bypassing an incomplete spinal cord injury. J. Neurosci. *34*, 13399–13410.

38. Courtine, G., Song, B., Roy, R.R., Zhong, H., Herrmann, J.E., Ao, Y., Qi, J., Edgerton, V.R., and Sofroniew, M.V. (2008). Recovery of supraspinal control of stepping via indirect propriospinal relay connections after spinal cord injury. Nat. Med. *14*, 69–74.

39. Lyu, D., Yu, W., Tang, N., Wang, R., Zhao, Z., Xie, F., He, Y., Du, H., and Chen, J. (2013). The mTOR signaling pathway regulates pain-related synaptic plasticity in rat entorhinal-hippocampal pathways. Mol. Pain *9*, 64.

40. Bateup, H.S., Johnson, C.A., Denefrio, C.L., Saulnier, J.L., Kornacker, K., and Sabatini, B.L. (2013). Excitatory/inhibitory synaptic imbalance leads to hippocampal hyperexcitability in mouse models of tuberous sclerosis. Neuron *78*, 510–522.

41. Luikart, B.W., Schnell, E., Washburn, E.K., Bensen, A.L., Tovar, K.R., and Westbrook, G.L. (2011). Pten knockdown in vivo increases excitatory drive onto dentate granule cells. J. Neurosci. *31*, 4345–4354.

42. Yamawaki, R., Thind, K., and Buckmaster, P.S. (2015). Blockade of excitatory synaptogenesis with proximal dendrites of dentate granule cells following rapamycin treatment in a mouse model of temporal lobe epilepsy. J. Comp. Neurol. *523*, 281–297.

43. Raab-Graham, K.F., Haddick, P.C., Jan, Y.N., and Jan, L.Y. (2006). Activity- and mTOR-dependent suppression of Kv1.1 channel mRNA translation in dendrites. Science *314*, 144–148.

44. Kauwe, G., Tsurudome, K., Penney, J., Mori, M., Gray, L., Calderon, M.R., Elazouzzi, F., Chicoine, N., Sonenberg, N., and Haghighi, A.P. (2016). Acute fasting regulates retrograde synaptic enhancement through a 4E-BP-dependent mechanism. Neuron *92*, 1204–1212.

45. Silver, J., and Miller, J.H. (2004). Regeneration beyond the glial scar. Nat. Rev. Neurosci. *5*, 146–156.

46. Chen, C.H., Sung, C.S., Huang, S.Y., Feng, C.W., Hung, H.C., Yang, S.N., Chen, N.F., Tai, M.H., Wen, Z.H., and Chen, W.F. (2016). The role of the PI3K/Akt/mTOR pathway in glial scar formation following spinal cord injury. Exp. Neurol. *278*, 27–41.

47. Inoki, K., Li, Y., Xu, T., and Guan, K.L. (2003). Rheb GTPase is a direct target of TSC2 GAP activity and regulates mTOR signaling. Genes Dev. *17*, 1829–1834.

48. Long, X., Lin, Y., Ortiz-Vega, S., Yonezawa, K., and Avruch, J. (2005). Rheb binds and regulates the mTOR kinase. Curr. Biol. *15*, 702–713.

49. Guo, X., Snider, W.D., and Chen, B. (2016). GSK3β regulates AKT-induced central nervous system axon regeneration via an eIF2Bε-dependent, mTORC1-independent pathway. eLife *5*, e11903.

50. Keppler-Noreuil, K.M., Parker, V.E., Darling, T.N., and Martinez-Agosto, J.A. (2016). Somatic overgrowth disorders of the PI3K/AKT/mTOR pathway & therapeutic strategies. Am. J. Med. Genet. C. Semin. Med. Genet. *172*, 402–421.

51. Saini, M.K., and Sanyal, S.N. (2012). PTEN regulates apoptotic cell death through PI3-K/Akt/GSK3β signaling pathway in DMH induced early colon carcinogenesis in rat. Exp. Mol. Pathol. *93*, 135–146.

52. Wu, D., Raafat, A., Pak, E., Clemens, S., and Murashov, A.K. (2012). Dicer-microRNA pathway is critical for peripheral nerve regeneration and functional recovery in vivo and regenerative axonogenesis in vitro. Exp. Neurol. *233*, 555–565.

53. Islamov, R.R., Hendricks, W.A., Jones, R.J., Lyall, G.J., Spanier, N.S., and Murashov, A.K. (2002). 17Beta-estradiol stimulates regeneration of sciatic nerve in female mice. Brain Res. *943*, 283–286.

54. Hamers, F.P., Lankhorst, A.J., van Laar, T.J., Veldhuis, W.B., and Gispen, W.H. (2001). Automated quantitative gait analysis during overground locomotion in the rat: its application to spinal cord contusion and transection injuries. J. Neurotrauma *18*, 187–201.